Combined Effects of Surface Dent and Residual Stress Generated by Shot Peening on Fatigue Properties of Induction Hardened Steel with Different Hardness

Shoichi Kikuchi[1], Keisuke Ono[2,*1], Koichiro Nambu[3] and Shogo Takesue[4]

[1]*Department of Mechanical Engineering, Faculty of Engineering, Shizuoka University, Hamamatsu 432-8561, Japan*
[2]*Department of Mechanical Engineering, Graduate School of Integrated Science and Technology, Shizuoka University, Hamamatsu 432-8561, Japan*
[3]*Department of Mechanical Engineering, Faculty of Engineering, Osaka Sangyo University, Daito 574-8530, Japan*
[4]*Department of Mechanical Engineering, Kyoto Institute of Technology, Kyoto 606-8585, Japan*

In this study, low alloy steel (AISI4140) specimens with different surface morphology and hardness were prepared by shot peening and fine particle peening, followed by induction hardening and tempering at different temperatures. Rotating bending fatigue tests were performed at stress ratio of -1 for these specimens, and the combined effects of the surface dent formed by peening and residual stress on the fatigue limit of the induction hardened steels were quantitatively investigated. It was found that the fatigue limit of the induction hardened steel tended to decrease with an increase in the size of the particles used in the peening. This was because fatigue cracks were initiated at the surface dents formed by peening. The parameter of surface morphology that showed a good correlation with the fatigue limit of the induction hardened steel was the waviness parameter which is corresponded to the size of surface dens formed by peening, but not the roughness parameter. Furthermore, a fatigue limit estimation for induction hardened steels with different surface morphology and hardness was described using a modified Goodman diagram. The improvement in the fatigue limit of steels with surface dents due to compressive residual stress was more significant as the hardness decreased, and the maximum fatigue limit improved by compressive residual stresses increased as the size of surface dents decreased. In contrast, the maximum value of the compressive residual stress that contributes to the increased fatigue limit of steels tended to increase as the hardness increased.

Keywords: *fatigue, shot peening, residual stress, hardness, induction hardening*

1. Introduction

Fatigue failure is the most common mode failure in mechanical components. Shot peening (SP) is widely used to improve the fatigue characteristics of metallic components as it can increase the surface hardness, generate compressive residual stress, and enhance grain-refinement. The effect of residual stress on the fatigue limit of surface-modified metallic materials can be expressed by modifying the fatigue limit diagram [1-5] because residual stress is regarded as the mean stress during the fatigue process. The effect of residual stress induced by shot peening on the fatigue limit of steels can be quantitatively estimated via the modified Goodman diagram.

However, it was reported that fatigue cracks in high-strength materials treated with peening were initiated at the surface dent induced by post-peening treatments [6-8]. In our previous work, only the effects of surface morphology on the fatigue limit of carburized steels with the same compressive residual stress and surface hardness have been investigated [9], wherein shot peening was performed as a pre-processing step before gas carburizing. The negative effects of surface morphology induced by shot peening on the fatigue limit should be quantitatively examined considering the positive effect of compressive residual stress generated by peening because the surface morphology and compressive residual stress depend upon the particle diameter used during peening.

In this study, the combined effect of surface morphology and residual stress induced by shot peening were investigated on the basis of a fatigue limit estimation for induction hardened and tempered steels with different hardness. The method was based on the combined results of fatigue tests, residual stress measurement, finite element method (FEM), observations of fracture surfaces, and tensile tests.

2. Experiment

2.1 Material and specimens

The material used in this study was AISI 4140 chromium-molybdenum steel with a Vickers hardness of 335 HV. Figure 1 shows the experimental procedures used: fabrication of specimens, electrochemical polishing (EP), fine particle peening (FPP), SP, and induction hardening. It was ensured that the formation of surface dents due to peening as a pre-processing step before induction hardening did not affect the residual stress and hardness of the surface of steels to quantitatively examine the effect of surface morphology on the fatigue limit of steels. Therefore, EP, FPP, and SP were conducted prior to the induction hardening of the hourglass-type specimens. After induction hardening, tempering was performed at 450 ºC or 100 ºC to change the specimen hardness (452HV or 743HV). Hereinafter, the tempered steels are referred to as the EP450, FPP450, SP450, EP740, FPP740 and SP740 series, respectively.

SP was performed on the specimens prior to induction hardening and tempering using spherical steel particles with a diameter and hardness of 600 μm and 700 HV, respectively. FPP was performed on the specimens prior to induction hardening and tempering using steel particles with a diameter of 50–150 μm. As results of observing the surface morphologies of the induction hardened and tempered specimens pre-treated with EP, FPP, and SP obtained using laser microscopy, the size of the surface dents increased with an increase in the shot particle diameter.

*1 Graduate Student, Shizuoka University

2.2 Testing

The residual stress was measured at the surface of the steels treated with peening using a portable X-ray device (type μ-X360s, Pulstec Industrial Co., Ltd.). Measurements based on the cosα method were conducted along the longitudinal direction of the minimum diameter of the hourglass-type specimens using a Cr Kα line generated at 30 kV and 1.5 mA. A diffraction plane of (211), corresponding diffraction angle of $2\theta = 156.4°$, and X-ray incidence angle of 35° were selected considering the properties of the target material. It was confirmed that the compressive residual stress generated at the surface of each specimen pre-treated with EP, FPP, and SP exhibited almost the same value because the compressive residual stress generated by SP and FPP as pre-treatment was released during the following induction hardening and tempering processes owing to the high temperature.

Rotating bending fatigue tests were performed at room temperature in air using a rotating bending fatigue testing machine at 1800 rpm. In this study, the fatigue limit (σ_w) was defined as the average of the maximum stress amplitude without specimen failure and the minimum stress amplitude at which the specimens failed, according to the Japan Society of Materials Science, Japan (JSMS) standard. The fractured surfaces of the failed specimens were observed using scanning electron microscopy (SEM) after testing.

3. Results and Discussion

3.1 *S-N* curves

Figure 2 shows the results of fatigue tests for the 450 series and 740 series. The fatigue limit of induction hardened and tempered steels was dependent upon the surface morphology and decreased with an increase in the shot particle diameter used for peening. As results of observing the fracture surfaces, every specimen failed from the surface dents formed by FPP or SP.

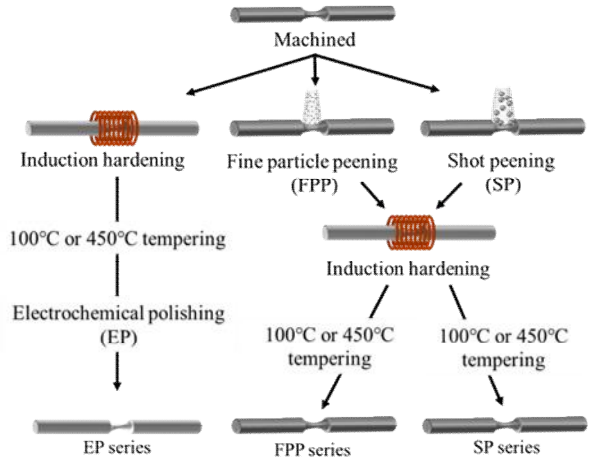

Figure 1 Schematic illustration showing the preparation of specimens with different surface morphology and hardness [10].

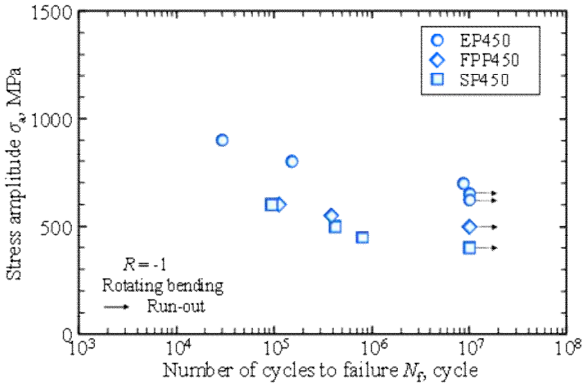

(a) 450 series

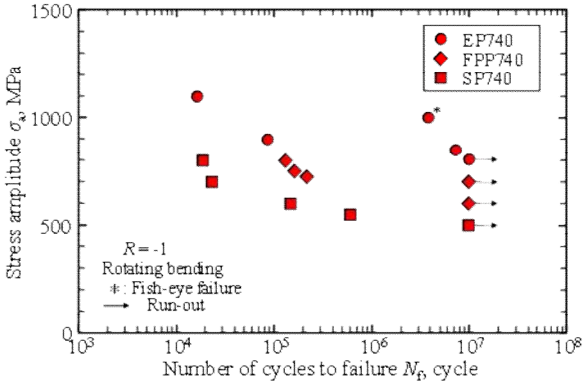

(b) 740 series

Figure 2 Results of rotating bending fatigue tests for the 450 series and 740 series [10].

3.2 Fatigue limit estimation

A fatigue limit estimation method for induction hardened and tempered steels according to the modified Goodman diagram was proposed to quantitatively evaluate the fatigue limit of steels with compressive residual stress and surface dents. In this diagram, the yield limit (σ_Y) was divided by the stress concentration factor (K_t), which was calculated by FEM, near the surface dent formed by peening because stress concentration decreases the yield strength of materials. In contrast, the tensile strength (σ_B) was not influenced by the stress concentration factor. In addition, the fatigue limit was decreased due to the presence of surface dents as shown in Figure 2. Therefore, the fatigue limit as a function of residual stress, which is regarded as mean stress, can be estimated for the induction hardened and tempered steels with surface dents induced by peening.

Figure 3 shows the fatigue limit diagram of the 450 series with different surface morphologies. Here, the *y*-axis indicates the stress amplitude (σ_a), whereas the *x*-axis indicates the sum of the mean stress and residual stress, i.e., $\sigma_m + \sigma_r$. In the case of rotating bending fatigue tests ($R = -1$), the *x*-axis value can be regarded as the residual stress (σ_r) because mean stress $\sigma_m = 0$. The fatigue limit estimation line in Figure 3 is drawn by connecting points α and β according to the modified Goodman diagram. Point α represents the ultimate tensile strength (σ_B = 1731 MPa), which is not influenced by the stress concentration. The *x*- and *y*-coordinates at point β represent the residual stress value of the specimen without fatigue failure after the fatigue tests ($N = 10^7$) and the fatigue limits of the EP450

(σ_w = 675 MPa), FPP450 (σ_w = 525 MPa), and SP450 (σ_w = 425 MPa). Therefore, the estimated fatigue limit increased with decreasing residual stress and increasing compressive residual stress; subsequently, it remained constant because the high compressive residual stress was released due to compressive yielding.

Figure 3 also revealed that the maximum fatigue limit improved by compressive residual stresses increased as the size of surface dents decreased. As a result of estimating the fatigue limit of the 740 series, it was found that the improvement in the fatigue limit of steels with surface dents due to compressive residual stress was more significant as the hardness decreased, and that the maximum value of the compressive residual stress that contributes to the increased fatigue limit of steels tended to increase as the hardness increased.

Consequently, the fatigue limit of the induction hardened and tempered steels with compressive residual stress and surface dents was quantitatively evaluated.

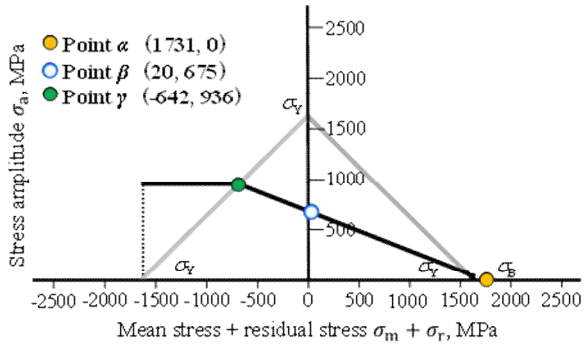

(a) EP450 series

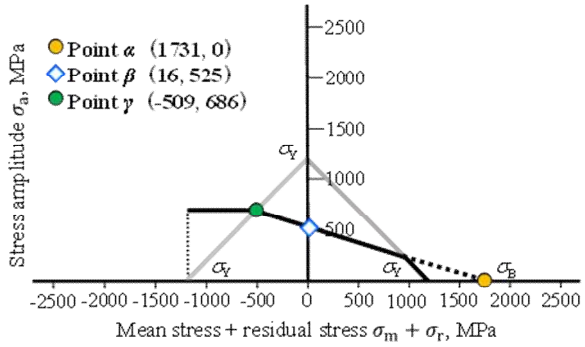

(b) FPP450 series

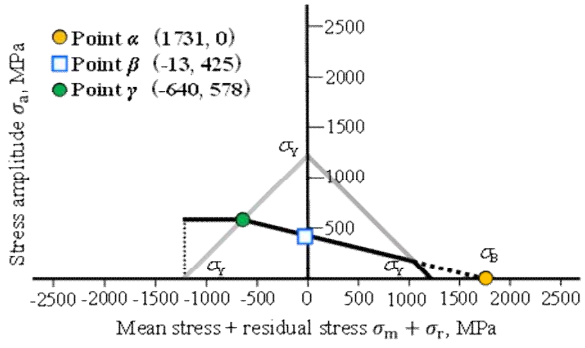

(c) SP450 series

Figure 3 Fatigue limit diagram for the 450 series considering the residual stress relaxation [10].

Conclusion

In this study, low alloy steel (AISI4140) specimens with different surface morphology and hardness were prepared by shot peening and fine particle peening, followed by induction hardening and tempering at different temperatures. Rotating bending fatigue tests were performed for these specimens, and the combined effects of the surface dent formed by peening and residual stress on the fatigue limit of the induction hardened steels were quantitatively investigated. It was found that the fatigue limit of the induction hardened steel tended to decrease with an increase in the size of the particles used in the peening. Furthermore, a fatigue limit estimation for induction hardened steels with different surface morphology and hardness was described using a modified Goodman diagram.

Acknowledgments

The authors would like to thank Mr. Toshiya Tsuji, Dr. Yuji Kobayashi (Sintokogio, Ltd.), and the Sectional Committee on Surface Modification for Fatigue of Materials (JSMS) for the technical support.

References

1) J. Arakawa, M. Kakuta, Y. Hayashi, R. Tanegashima, H. Akebono, M. Kato and A. Sugeta: Surf. Eng. **30** (2014) 662-669.
2) J. Arakawa, T. Hanaki, Y. Hayashi, H. Akebono and A. Sugeta: Mater. Sci. Eng. A **43** (2020) 211-220.
3) K. Minamizawa, J. Arakawa, H. Akebono, K. Nambu, Y. Nakamura, H. Hayakawa and S. Kikuchi: Int. J. Fatigue **160** (2022) 106846.
4) R. Fueki, K. Takahashi and K. Houjou: Mater. Sci. Appl. **6** (2015) 500-510.
5) S. Kikuchi, K. Minamizawa, J. Arakawa, H. Akebono, S. Takesue and M. Hayakawa: Int. J. Fatigue **168** (2023) 107441.
6) T. Morita, A. Miyashita, S. Kariya, M. Kumagai, S. Takesue and J. Komotori: Results Mater. **7** (2020) 100128.
7) T. Morita, A. Miyatani, S. Takesue, M. Kumagai and J. Komotori: Mater. Trans. **62** (2021) 1298-1303.
8) Y. Nakamura, K. Nambu, T. Akahori, T. Shimizu and S. Kikuchi: Appl. Sci. **11** (2021) 4307.
9) K. Minamizawa, S. Takesue, K. Nambu, Y. Nakamura, H. Akebono and S. Kikuchi: J. Jpn Soc. Abras. Technol. **66** (2022) 149-153.
10) K. Ono, K. Nambu, S. Takesue and S. Kikuchi: J Soc. Mater. Sci. Jpn. **72** (2023) in press.